Effect of Mg Doping on Structural and Optical Properties of Al-Mg Co-doped ZnO Thin Films Deposited via Sol-gel Technique

El Hamidi A[1]*, Chaik M[2], Jannane T[3], Meziane K[1], El Hichou A[1] and Almaggoussi A[1]

[1]Groupe d'Etude des Matériaux Optoélectroniques (GEMO), FST Marrakech, University Cadi Ayyad, BP549, Av. A. Khattabi, Marrakech, Morocco

[2]Laboratory of Nanomaterials, Energy and environment (LN2E), University Cadi Ayyad, Marrakech, Morocco

[3]Laboratory of material physics, Sultan Moulay Sliman University, Sciences and technologies Faculty, BP 523, 23000 Beni Mellal, Morocco

Research Article

ABSTRACT

Aluminium doped and (Mg-Al) co-doped zinc oxide thin films were deposited by sol-gel technic from aqueous solution onto glass substrates at optimum conditions. The variations of the structural, electrical and optical properties with the doping and co-doping concentration were investigated. XRD analysis showed typical patterns of the hexagonal ZnO structure for all films and AMZO thin films exhibited preferred orientation growth along the c-axis. No diffraction peaks of any other structure were found. The grain size, texture coefficient and optical band gap values were evaluated for different aluminum concentrations and (Mg-Al) co-doping ratio. The results show that increasing the Mg content, the films improve their crystallinity with the (002) preferred orientation and the transmittance reaches 85%. The optimized results were obtained for co-doped (Mg-Al) concentration at ratio of 2/1.

INTRODUCTION

Zinc oxide (ZnO) is a semiconducting material with more important and interesting properties than most other materials. It is a II–VI compound semiconductor whose ionicity resides at the borderline between the covalent and ionic semiconductors. The significant properties of ZnO are: a direct band gap (3,4 eV) at room temperature, high exciton binding energy (60 meV) [1], which is much greater than ZnSe (20 meV) and GaN (25 meV), high optical transparency in the visible region and low electrical resistivity. The higher exciton binding energy enhances the luminescence efficiency. Non-toxicity and abundance of ZnO on earth makes it an ideal candidate used as a transparent electrical contact for solar cells in thin layers.

Owing to these properties, ZnO becomes a very promising material for many practical applications such as a transparent conductive contact [2], thin films gas sensors [3,4], varistors [5], surface acoustic wave devices [6], U.V laser [7], luminescent materials [8], an n-type conducting window in thin film solar cells based on cadmium telluride [9] or indium diselenide [10] and others.

Several technics have been used for fabrications of ZnO thin films such as physical vapor deposition (PVD) [11], magnetron sputtering [12], spray pyrolysis [13], Chemical vapor deposition (CVD) [14] electrochemical deposition and sol–gel processing [15]. Among these technics, sol–gel attracted more interests because of its great advantages: simplicity, low cost, large area substrate

coating and easy to realize doping incorporation.

The Applications of ZnO can be improved by suitable dopant as physical and optical properties depend upon the dopant and synthesis conditions. Note that several dopants have been tested by different technics growth process for ZnO. In most cases, the purpose of the doping is to modulate the optical and or electrical properties of ZnO thin films. Dopants such as Al, Ga, In, B, Ag, and Cl were all expected to enhance the native n type conductivity of ZnO [16-22]. Dopants like Cd, Mg have been shown to modify the optical properties of ZnO by changing its band gap [23]. All single doped ZnO thin films could not improve simultaneously the physical and optical properties. Co-doping is an alternative and effective method to increase these properties simultaneously of ZnO thin films [24-26]. Traditionally co-doping in ZnO thin films has been prepared by using the combination of the groups III elements with groups VI elements. However, the combination of Al-Mg has not been widely explored. Many papers report on the physical properties of co-doped ZnO, most of them fixed one dopant by varying the second dopant. But our studies concern to fix the dopant ratio (Mg, Al) /Zn= 5%.

In this paper, we deposited Al-Mg-ZnO thin films on glass substrate via sol-gel mediated spin coating methods. The main goal of this study was to investigate the effect of Al-Mg co-doping on structural, surface morphology and optical properties of AMZO thin films.

EXPERIMENTAL SECTION

Al doped ZnO: AZO

The ZnO thin films doped with Al were deposited on glass substrates via sol-gel spin coating technic. Zinc acetate dehydrate [Zn $(CH_3OO)_2.2H_2O$] (Aldrich 99%), was used as a starting material. 2-methoxyethanol $(C_3H_8O_2)$, monoethanolamine (MEA), aluminum nitrate nanohydrate [Al$(NO_3)_3.9H_2O$] was used as solvent, stabilizer and dopant respectively. The concentration of the solutions was maintained at 0.75 mol/l. We prepared four samples with different Al doping percentage (1%, 3%, 5% and 7%) (**Table 1**).

Mg, Al Co-doped ZnO: AMZO

The ZnO thin films co-doped with Mg and Al were also deposited on glass substrates via sol-gel spin coating technique. Zinc acetate dehydrate [Zn $(CH_3OO)_2.2H_2O$] was used as a starting material. 2-methoxyethanol $(C_3H_8O_2)$, monoethanolamine (MEA), aluminum nitrate nanohydrate [Al$(NO_3)_3.9H_2O$] and magnesium acetate [Mg$(CH_3COO)_2.4H_2O$] were used respectively as solvent, stabilizer and dopants. The concentration of the solutions was maintained at 0.75 mol/l and the concentration of doping was considered constant noting that (Mg, Al)/Zn=5% and the contents of Al and Mg were varied. With this approach, six samples were prepared at different ratio.

The Al doped ZnO and Mg–Al co-doped ZnO films were deposited on the glass using the spin coating technique. First, the glass substrates were ultrasonically cleaned in acetone and rinsed in deionized water. Next, the obtained sols were poured onto a glass substrate and spin coated. Finally, the films were air dried at 150°C and annealed at 500°C for one hour. The prepared thin films were examined by X-ray diffraction (XRD, D/Max-2400) to analyze their crystal structure. A scanning electron microscope (SEM, JSM-6701F) was used to explore surface morphology. The transmittance spectra of the UV–visible light passing through the films were measured by a UV–visible spectrophotometer (Lambda35 UV/VIS) in order to study the optical properties of studied samples.
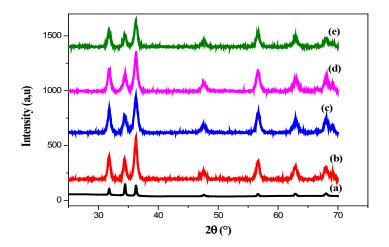
RESULTS AND DISCUSSIONS

Al Doped ZnO=AZO

Structural and morphological characterizations: Figure 1 shows the X-ray diffraction patterns of ZnO films doped with different concentrations of aluminum. XRD results revealed that all samples of ZnO doped Al, crystalized with wurtzite structure and exhibit tree peaks characteristic of ZnO corresponding to (100), (002), and (101) places at 2θ=31,85°, 34,59° and 36,42° respectively and minor peaks at 2θ=47,62°, 56,75°, 63,13° and 68,08° corresponding respectively to (102), (110), (103) and (112) plans. For the undoped ZnO film, the strong intensity of (002) plan compared to (101) or (100) orientation plane suggests that the ZnO have a preferential (002) orientation with the c-axis perpendicular to the substrate surface. Furthermore, for the Al doped ZnO thin film, the (101) peak was increased indicating on more favorable of the (101) film orientation. Similar results are observed in the literature [26] but El Hichou et al. [27] and Trolio et al. [28] reported that the films had a preferred orientation with c-axis perpendicular to the substrate. In addition, for AZO, lattice parameters a and c of different samples were not sensitive to the Al-doping (**Table 1**). No secondary phases related to impurity phases were detected in the AZO films which support that Zn ions were substituted by Al sites entire the lattice of ZnO crystal.

Figure 1. X-ray pattern of Al doped ZnO films, at various percentage, deposited on glass substrates by sol gel (a) C_{Al}=0%, (b) C_{Al}=1%, (c) C_{Al}=3%, (d) C_{Al}=5% and (e) C_{Al}=7%.

The grain size of different samples was determined from XRD diffraction spectra, using the Scherrer relationship [29] (**Table 1**). **Figure 2** shows the evolution of the grain size with different Al concentration. The grain size decreases with increasing the Al content and it ranges from 33.5 nm and 15 nm for the (002) plan. This decrease in the crystallite size of AZO films is attributed to the smaller ionic radii of Al than Zn.
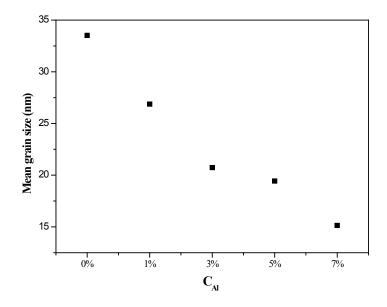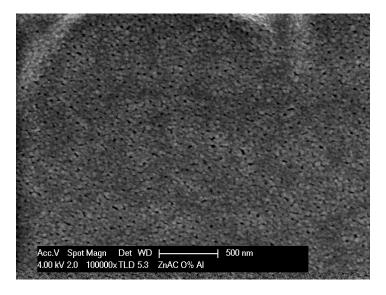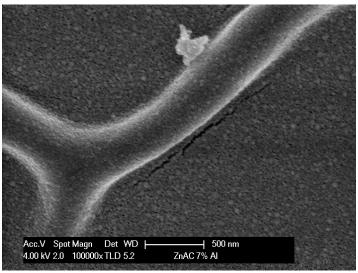

Figure 2. Grains size as function of Aluminum salt concentration of AZO thin films deposited on glass substrate by sol gel.
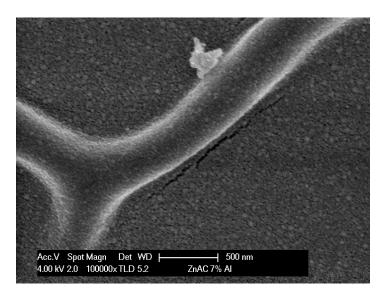
Table 1. Lattice parameters and crystallite size of AZO films deposited on glasses substrate by sol gel and prepared for different concentration of Al.

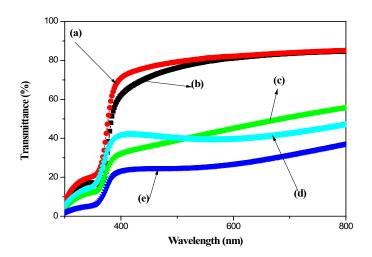| Sample	Al content	a (Å)	c (Å)	d (nm)
ZO	Undoped	3.25	5.21	33,525
A1ZO	1%	3.249	5,207	26.8783
A3ZO	3%	3,248	5.2066	21.235
A5ZO	5%	3.247	5.2064	19.43
A7ZO	7%	3.2447	5.2063	15.1349

Figure 3. SEM images of AZO films deposited on glasses substrate by sol gel and prepared at various aluminum concentration. (a) C_{Al}=0%, (b) C_{Al}=1% and (c) C_{Al}=7%.

Scanning microscopy observations were used to analyze morphology of the studied samples and determining the particle size. The morphologies of ZnO thin films prepared in solutions with different concentrations of aluminum content are shown in **Figure 3**. It's clearly shown that there is a change in the surface morphology of ZnO films with increasing the concentration of the Al dopant. The SEM images of the undoped ZnO films depicts a microstructure that consists of hexagonal like grains of ap-

proximately 35 nm in size. As the Al doping increased, the surface of AZO thin films exhibited smoother surfaces and smaller grain sizes. Al-doping concentration up 7% shows a deterioration of the crystallinity of the films which may be due to the stress induced by the difference in ionic size between Zn and Al dopant.

Optical properties: The optical transmittance is an important optical parameter for transparent conducting oxides. Optical transmittance spectra of undoped and Al-doping ZnO films showed that all films are transparent in the visible regions (**Figure 4**). Up 3% of Al concentration, the films become whitish in appearance resulting in the decrease of the transmittance of the layers.

Figure 4. Transmission spectra vs. wavelength of AZO films deposited on glasses substrate by sol gel and prepared at various aluminum concentration. (a) CAl=0%, (b) CAl=1%, (c) CAl=3%, (d) CAl=5% and (e) CAl=7%.

The energy band gap (E_g) could be calculated by assuming a direct transition between the valence band (E_v) and the conduction band (E_c) by using the following equation:

$$\alpha.h\nu = A.(h\nu - E_g)^{1/2}$$

Where A is a constant, hν is the photon energy and E_g is the band gap for the direct band gap semiconductor. The optical band gap was obtained by extrapolating the linear part of curves $(\alpha.h\nu)^2$ as a function of incident photon energy hν to intercept the energy axis. The dependence of E_g on Al-doping is reported in **Figure 5**. The effect of Al-doping is to increase E_g values up to 3.19 eV and 3.22 eV for 1% and 7% doped films respectively. With the increasing Al doping level, the optical band gap of films is growing, which causes the absorption edge shift to short wavelength region. The band gap of AZO thin films was greater than that of undoped film. The increase in the band gap of Al-doped ZnO films has been reported earlier also [30-32] and this has been attributed to the Burstein-Moss effect. The Al atoms donor provide additional carriers which cause the Fermi level to move into the conduction band, so the band gap becomes larger.
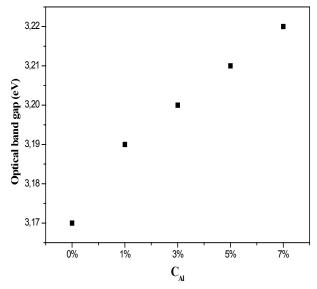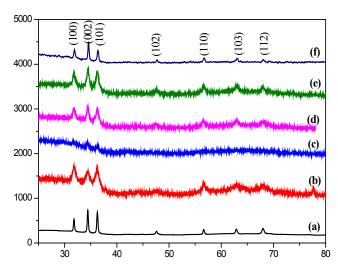

Figure 5. Optical band gap as function of Aluminum salt concentration of AZO thin films deposited on glass substrate by sol gel.

Al, Mg Co-doped ZnO: AMZO

Structural and morphological characterizations: Figure 6 shows the XRD patterns of undoped, doped and co-doped ZnO thin films. All diffractive peaks can be indexed into the ZnO hexagonal wurtzite structure, indicating that Mg and Al doping did not change the wurtzite ZnO structure. Bragg reflections with 2θ values of 31,85°, 34,59° and 36,42° which were assigned to the diffractions from (100), (002) and (101) planes. Minor peaks (102), (110), (103) and (112) planes corresponding to 2θ values of 47,62°, 56,75°, 63,13° and 68,08° were also detected. Further, there are no additional reflection indicating that no secondary phases were founded. This result indicated that Mg^{2+} and Al^{3+} ions were substituted into Zn^{2+} ion sites or incorporated into interstitial sites in the ZnO lattice. The growth along (002) lattice direction exhibited the strongest intensity indicating the preferential growth of hexagonal wurtzite crystal structures along crystallographic c-axis [33,34]. The incorporation Mg in the compound causes reorientation as shown by the relative increase of the (002) peak intensity.
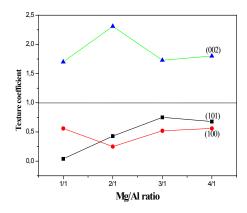

Figure 6. X-ray pattern of ZnO, Al-ZnO, Mg-ZnO and (Mg-Al) co-doped ZnO films deposited on glass substrates by sol gel. (a) ZnO, (b) CAl=5%, (c) Mg/Al=2/1, (d) Mg/Al=3/1, (e) Mg/Al=4/1 and (f) CMg=5%.

The crystallinity structures of the films are shown depending on the increasing of Al/Mg ratio. With increasing Mg concentration, the intensity of the (002) peak increases and FWHM values of this peak increases. The broadening of the XRD indicated an excellent crystallinity of AMZO.

We have studied the influence of Al/Mg ratio on the film texture of plane (002), by calculating the texture coefficient T_c according the following formula [35]:

$$T_C = \frac{I_{(hkl)}}{\frac{1}{n}\acute{O}I_{(hkl)}}$$

The calculated texture coefficient T_c are presented in **Figure 7**. AMZO films have larger T_c values for (002) plane suggesting that all the films co-doped with (Al-Mg) have c-axis preferred orientation. Moreover, the high T_c value and the higher grain size (30,17 nm), was obtained for the film A2MZO (with 2/1 ratio), indicating a good crystallization along the growth c-axis. This confirms the XRD results.

Figure 7. Texture coefficient plot of the (002), (100) and (101) peak versus Mg/Al ratio of AMZO films deposited on glass substrate by sol gel.

The overall structures of AMZO thin films are affected by the strain due to Mg/Al substitution in the ZnO lattice. The stress state in the layer can be determined from the XRD analysis. According to the biaxial stress model, the stress ε along the c-axis perpendicular to the plane of the substrate is calculated from the parameter c [36]:
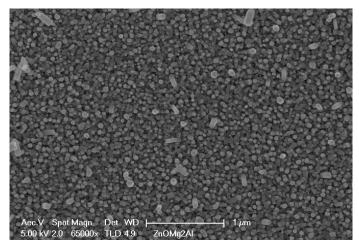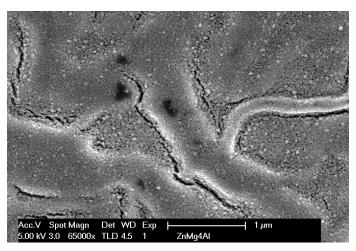
$$\varepsilon = \frac{C_{film} - Co}{C_0}$$

where C is the lattice constant of the layer and C_0 is the lattice constant of the layer without stress (C_0=0.5206 nm [24]). The sign of this parameter indicates that the layer has undergone a compressive stress (negative) or in an extensive stress (positive) depending the orientation of the layer growth (c-axis). The values of ε along the (002) plane for all films AMZO are listed in **Table 2**. All the strain values are found to be positive (extensive or tensile in nature). For pure ZnO, the stresses have origin of deposition technique and temperature of the substrate. For AZO, the value of ε is very weak. This phenomenon is explained by occupation of the substitutional sites by the Al ions knowing that $r_{Zn2+} > r_{Al3+}$. For AMZO films, the stress increased because of occupation of the substitutional sites by the Mg ions knowing that $r_{Zn2+} < r_{Mg2+}$. The small residual stress of AMZO thin films was found to be 0.568 GPa when the Al/Mg ratio was 2/1.

Table 2. Stress of AZO and AMZO films Co-doped (Mg-Al) with various contents and deposited on glasses substrates by sol gel.

Samples	ZO	AZO	AMZO	AM2ZO	AM3ZO	AM4ZO	MZO
Stress in GPa	0.768	0.31	0.384	0.568	2.689	2.689	2.75

The morphologies of AMZO thin films are shown in **Figure 8**. These SEM images clearly show that there is a change in the surface morphology of ZnO films due to the (Al-Mg) co-doping. Note that the grain size decreases with increasing Mg concentration up to 2/1 and saturates at higher concentrations (**Table 3**). The film deposited at 2/1 consists of hexagonal like grains of approximately 30,17 nm. The decrease of particle size could be caused by the smaller ionic radius of Mg^{2+} (0.066 nm) and Al^{3+} (0.053 nm) compared with Zn^{2+} (0.074 nm). When the Mg/Al ratio is up 2/1, the mean size of hexagonal like grains decreases and more cracks are present in the films. This result is in good agreement with XRD data and affirms once again an improvement in the films crystallinity for co-doping ratio 2/1.
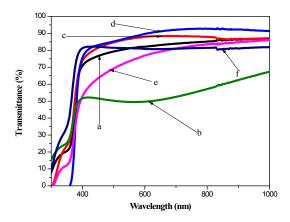

Figure 8. SEM images of AMZO films deposited on glasses substrate by sol gel and prepared at various Mg/Al ratio. (a) Mg/Al=2/1 (b) and (b) Mg/Al=4/1.

Table 3. Lattice parameters and crystallite size of AMZO films deposited on glasses substrate by sol gel and prepared for different Mg/Al ratio.

Sample	Mg/Al ratio	a (Å)	c (Å)	d (nm)
ZO	Undoped	3.25	5.21	33,525
AZO	0/1	3.2447	5,2064	19,43
AM1ZO	1/1	3,2464	5.208	26,43
AM2ZO	2/1	3.2499	5.2085	30.17
AM3AZO	3/1	3.2447	5.22	28.18
AM4AZO	4/1	3.2447	5.22	29.30
MZO	5/0	3,2355	5.22	32,38

Optical properties: Figure 9 shows the transmittance spectra of ZnO, AZO, MZO and AMZO thin films. The spectra show that all the films have sharp ultraviolet absorption edges in the UV region. The introduction of Al causes a sharp decrease of transmission as can be seen by comparing the results of ZnO and AZO samples first. When the Mg atoms have been introduced, AMZO thin films show higher transparency than the other films and increases to its maximum for 2/1 and 3/1 ratios. For Mg contents even greater, optical transmission decreased while remaining superior to that of the AZO sample. In the visible region (400-800 nm) the samples having 2/1 and 3/1 ratios show the best transmission reaching 85%. As a result, the excellent transparency of those samples allows for a clear minimization of the visible light losses, and then an improvement of solar energy harvesting. These results are in agreement with those of XDR and SEM.

Figure 9. Transmission spectra vs. wavelength of AMZO films deposited on glasses substrate by sol gel and prepared at various Mg/Al ratio. (a) ZnO; (b) CAl=5%, (c) Mg/Al=2/1, (d) Mg/Al=3/1, (e) Mg/Al=4/1 and (f) CMg=5%.

The bandgap (E_g) as a function of (Al-Mg) co-doping content is shown in **Figure 10**. The bandgap of AMZO thin films was superior than that of pure ZnO thin films. Furthermore, the bandgap of AMZO thin films increases with increasing Mg/Al ration. The increasing of the bandgap for AMZO thin films has been attributed to the Fermi level moving into the conduction band caused by the increase of carrier concentration in AMZO thin films because of the substitution of the Al and Mg ions into Zn ion sites. When electrons located at the valence band require an additional energy to be excited to higher energy states in the conduction band, the optical band gap is increased. Similar results have also been reported [37,38]. Another explication had cited by Rouchdi et al. [39]. They have related this increasing of band gap in to the defects created after Mg^{2+} substitution for Zn^{2+} and then enters the ZnO lattice due to variation in their ionic radius. This finding is in agreement with those of XDR and SEM.
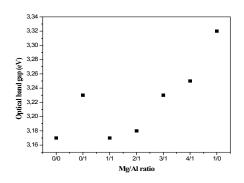

Figure 10. Optical band gap as function of Mg/Al ratio of AMZO thin films deposited on glasses substrate by sol gel.

CONCLUSION

Transparent films of aluminum-doped and (Mg-Al) co-doped zinc oxide have been deposited by sol gel technique at optimum conditions in glass substrate. The influence of Al doping and (Mg-Al) co-doped on the physical properties was found to be significant. The structural and morphological studies revealed that all films are polycrystalline and (Mg, Al) exhibit a preferential orientation along the [002] direction with preferred c-axis orientation. The adding of Mg in all the samples changed the nucleation and growth mechanism of AMZO. Furthermore, addition of Mg improves the transmittance, further increase the optical gap. The optical band gap energy revealed the variation from 3.17 to 3.25 eV with increased Al/Mg ration which is attributed to the Burstein-Moss effect. The films synthetized at 2/1 (Mg, Al) co-doped ZnO showed a high transmittance of 85% at λ=500 nm with an optical band gap at 3.2 eV.

The produced highly transparent AM2ZO thin films at optimum conditions may be useful for specific applications as transparent n-type windows in solar cells for sensor devices where large surface areas are needed.

REFERENCES

1. Mihailovic M, et al. Optical and excitonic properties of ZnO films. Opt Matt 2009;31:532-536.

2. Lai LW and Lee CT. Investigation of optical and electrical properties of ZnO thin films. Mater Chem Phys 2008;110:393-396.

3. Xu J, et al. Sensors and Actuators B: Chemical. Sens Act B Chem 2000;66:277-279.

4. Gómez-Pozos H, et al. Cu-Doped ZnO thin films deposited by a sol-gel process using two copper precursors: Gas-sensing performance in a propane atmosphere. Materials 2016;9:87.

5. Gupta TK. Application of Zinc Oxide Varistors. J Am Ceram Soc 1990;73:1817-1840.

6. Bock J, et al. Characterization of undoped and Cu-doped ZnO films for surface acoustic wave applications. Thin Solid Films 2001;398-399:641-646.

7. Tang ZK, et al. Room-temperature ultraviolet laser emission from self-assembled ZnO microcrystallite thin films. Appl Phys Lett 1998;72:3270.

8. Raji R and KG Gopchandran. ZnO nanostructures with tunable visible luminescence: Effects of kinetics of chemical reduction and annealing. J Sci: Adv Mater Dev 2017;2:51-58.

9. Major J, et al. Development of ZnO nanowire based CdTe thin film solar cells. Sol Energy Mater Sol cells 2017;160:107-115.

10. Yousfi EB, et al. Cadmium-free buffer layers deposited by atomic later epitaxy for copper indium diselenide solar cells. Thin Solid Films 2000;361-362:183-186.

11. Jimenez-Cadena G, et al. Synthesis of different ZnO Nanostructures by modified PVD process and potential use for dye sensitized solar cell. Matt Chem Phys 2010;124:694-698.

12. Zhouy Y and Kelly PJ. The properties of tin-doped indium oxide films prepared by pulsed magnetron sputtering from powder targets. Thin Solid Films 2004;469:18-23.

13. El Hichou A, et al. Influence of deposition temperature (Ts), air flow rate (f) and precursors on cathodoluminescence properties of ZnO thin films prepared by spray pyrolysis. J Lum 2005;113:183-190.

14. Purica M, et al. Optical and structural investigation of ZnO thin films prepared by chemical vapor deposition (CVD).Thin Solid Films 2002;403-404:485-488.

15. Hussein HF, et al. Preparation ZnO Thin Film by using Sol-gel-processed and determination of thickness and study optical properties. J Mater Environ Sci 2011;2:423-426.

16. Singh AV and Mehra RM. Highly conductive and transparent aluminum-doped zinc oxide thin films prepared by pulsed laser deposition in oxygen ambient. J Appl Phys 2001;90:5661.

17. Bhosle V, et al. Electrical properties of transparent and conducting Ga doped ZnO. J Appl Phys 2006;100:033713.

18. Yuan GD, et al. Tunable n-Type Conductivity and Transport Properties of Ga-doped ZnO Nanowire Arrays. Adv Mater 2008;20:168-173.

19. Luna-Arredondo EJ, et al. Indium-doped ZnO thin films deposited by the sol–gel technique. Thin Solid Films 2005;490:132-136.

20. Pawar BN, et al. Deposition and characterization of transparent and conductive sprayed ZnO:B thin films. J Phys Chem Solids 2005 ;66:1779-1782.

21. Rouleau C, et al. Growth of highly doped p-type ZnTe films by pulsed laser ablation in molecular nitrogen. Appl Phys Lett

1995;67:2545-2547.

22. Gonzalez-Penguelly B, et al. New infrared-assisted method for sol-gel derived ZnO:Ag thin films: Structural and bacterial inhibition properties. Mater Sci Eng C 2017;78:833-841.

23. Wang YS, et al. Nanocrystalline ZnO with Ultraviolet Luminescence. *J Phys Chem B* 2006;110:4099-4104.

24. Al-Ghamdi AA, et al. Semiconducting properties of Al doped ZnO thin films. Spectrochimica Acta Part A: Molecular and Biomolecular Spectroscopy 2014;131:512-517.

25. Hai-Yan He. Enhancing Optical and Electrical Properties of La- and Al-Codoped ZnO Thin Films Prepared by Sol-Gel Method -La Codoping Effect. Recent Pat Nanotechnol (United Arab Emirates) 2017;11:146-153.

26. Hayder J, et al. Gallium contents-dependent improved behavior of sol–gel-grown Al:Ga co-doped ZnO nanostructures. Appl Phys A 2017;123:665.

27. El Hichou A, et al. Influence of the aluminum incorporation on the properties of electrodeposited ZnO thin films. Surf Coat Technol 2015;270:236-242.

28. Trolio AD, et al. Blueshift of optical band gap in c-axis oriented and conducting Al-doped ZnO thin films. J Appl Phys 2009;105:113109.

29. Ibrahim AA, et al. Structural and electrical properties of evaporated ZnTe thin films. Vacuum 2004;75:189-194.

30. Fang D, et al. Influence of Al doping on structural and optical properties of Mg–Al co-doped ZnO thin films prepared by sol–gel method. J Alloys Comp 2014;589:346-352.

31. Zhai CH, et al. Effects of Al doping on the properties of ZnO thin films deposited by atomic layer deposition. Nanoscale Res Lett 2016;11:407.

32. Duan L, et al. Structural, optical and photocatalytic properties of (Mg,Al)-codoped ZnO powders prepared by sol–gel method. J Phy. Chem. Sol. 2015;76:88-93.

33. Shinde SS, et al. Physical properties of transparent and conducting sprayed fluorine doped zinc oxide thin films. Sol Sta Sci 2008;10:1209.

34. Tüzemen ES, et al. Dependence of film thickness on the structural and optical properties of ZnO thin films. Appl Surf Sci 2009;255:6195-6200.

35. Ramakrishna KT, et al. Highly oriented and conducting ZnO: Ga layers grown by chemical spray pyrolysis. Surf Coat Technol 2002;151-152:110-113.

36. Lee KE, et al. Structural, electrical and optical properties of sol–gel AZO thin films. Cur Appl Phys 2009;9:683-687.

37. Smith AM and Nie S. Semiconductor nanocrystals: structure, properties, and band gap engineering. Acc Chem Res 2010;43:190-200.

38. Hartnagel H. Semiconducting transparent thin films. CRC Press, 1995.

39. Rouchdi M, et al. Synthesis and characteristics of Mg doped ZnO thin films: Experimental and ab-initio study. Results Phys 2017;7:620.